Chapter 4

Kinematics of the Cometary Globules

4.1 Introduction

In this chapter we interpret the radial velocities measured for the heads and along the tails of the cometary globules. We first deduce a morphological center for the distribution of the CGs. Then the distance estimate is discussed. These steps are necessary to remove systematic effects like galactic rotation and for the interpretation of the velocities.

4.2 The center of the distribution of the CGs

For any assumed center, the tail position angle θ_{TH} with respect to the line joining the head and the center can be calculated using spherical geometry, as illustrated in figure 4.1. The center and the head of a CG can be joined by a great circle on the celestial sphere. The tail forms a part of another great circle. The angle between these two great circles is what we want. The equation for a great circle is

$$\tan 6 = \sin(\alpha - \alpha_0) \tan i \tag{4.1}$$

where α_0 is the point of intersection of the great circle and the celestial equator and i is the inclination between the great circle and the celestial equator. We can find α_0 and i for the the two great circles: one formed by joining the center and the head and the other being the great circle of which the tail forms a part. Let us call them α_{0h}, i_h and α_{0t}, i_t. In the spherical triangle ABC (refer to figure 4.1) we are interested in A, which is θ_{th}. By the four parts formula (Smart 1977),

$$\mathrm{b} = \cot^{-1}((\cos \mathrm{a} \cos \mathrm{C} + \sin c \sin C)/\sin a) \tag{4.2}$$

Then from the sine formula

$$\theta_{th} = A = \sin^{-1}(\sin B \sin a / \sin b) \tag{4.3}$$

where

$$a = \alpha_{0t} - \alpha_{0h}$$

$$B = i_h \; ; \; C = \pi - i_t \text{ if } \alpha_{0h} > \alpha_{0t} \text{ and}$$

$$B = i_t \; ; \; C = \pi - i_h \text{ if } \alpha_{0h} < \alpha_{0t}.$$

To identify a center for the CG system we associate with every point in the central region a fraction f, defined as the fraction of CGs with θ_{TH} (calculated using that

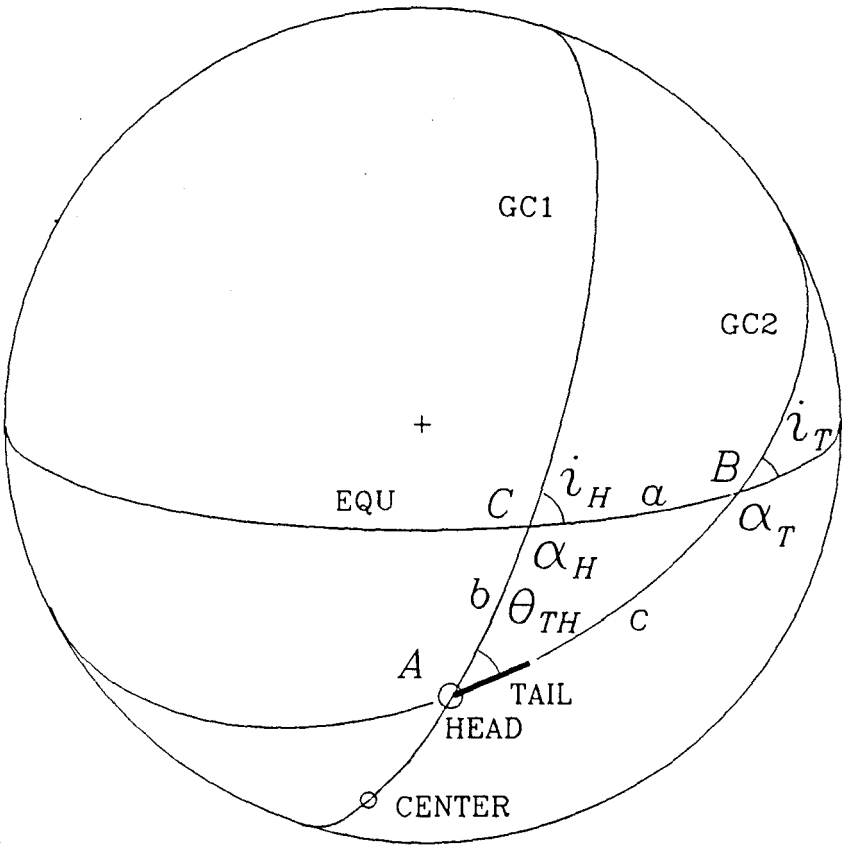

Figure 4.1: Geometric constructions used for deriving the tail position angle θ_{TH} relative to the line joining the head and any assumed center for a CG. GC1 is the great circle on the celestial sphere of which the line joining the center and the head of a CG forms a part. GC2 is the great circle of which the tail forms a part. GC1 and GC2 are characterised by (α_H, i_H) and (α_T, i_T), the RAs at which the great circles intersect the equator and their inclinations to the equator. θ_{TH} is the angle between these two great circles.

point as the center) within ± 10°. We evaluated f over a 15° × 15° area in the central region with grid points separated 0.5° in both a and 6. Figure 4.2 shows a contour plot of j. Only those CGs have been used for which we have measured the co-ordinates. CG24 has riot been included because of its anomalous tail direction. The CGs used in the analysis are shown as filled circles with tails and the CGs not used are shown as open circles with tails. For clarity tlie tail lengths shown have been scaled up 10 times. The contour spacing is 0.05 with every third contour drawn as a solid line. One can see that there is a central maximum with which 60% of the CGs are associated. The locations of the various interesting objects such as ζ Pup, γ^2 Vel, the Vela SNR etc. are also marked in tlie figure. The SNR Puppis A lies very close to the center but we show in the next section that it is very unlikely to be associated with the CGs. There are no strong local maxima associated with any of these objects. This indicates that most CGs are affected by a combination of objects rather than a particular one. The co-ordinates of the central maximum are $\alpha = 8^h\ 17^m$, and $6 = -43^o$. We will refer to this point as the *morphological* center or *center* for short, hereafter. The center deduced by us is 1.5° north of *center1* of Z83. Reducing the limiting θ_{TH} from ±10° to ±5° for calculating f merely results in increased noise on the contour plot. The apparently anomalous CG24 tail can be understood by noticing that it is so close to *center* that even small errors in the location of center can make the tail direction look anomalous.

4.3 Is Puppis A associated with the CGs?

In view of the remarkable near coincidence of tlie deduced *center* with the SNR Puppis A, it is worth briefly discussing whether the two may be causally connected. Zarnecki et *al.*(1978) estimate a distance of 1 kpc for Puppis A from X-ray absorption measurements. The $\Sigma - D$ distance to Puppis A is 2-2.5 kpc (Milne,1979,Casewell & Lerche,1979) although it should be emphasised that this method has been severely criticised in tlie literature (Srinivasan and Dwarakanath 1982; Green 1984). The latest estimate based on the kinematic distance to molecular clouds interacting with Puppis A gives 2.2 kpc (Dubner & Arnal,1988). We will therefore adopt a distance of 2 kpc to Puppis A. At this distance it would be very difficult to detect CGs, especially ones close to the galactic plane. If the CGs are placed at the estimated distance to Puppis A, then they will be ≈ 200 pc away from the SNR. From the size of the SNR it is clear that the SN shock has not reached the CGs. So the only way Puppis A may be associated with the formation of the CGs is through the photon pulse at the time of the explosion or alternatively the UV radiation and stellar wind from its *progenitor*. The age of Puppis A has been estimated to be ∼ 3700 yrs (Winkler et *al.*,1988).

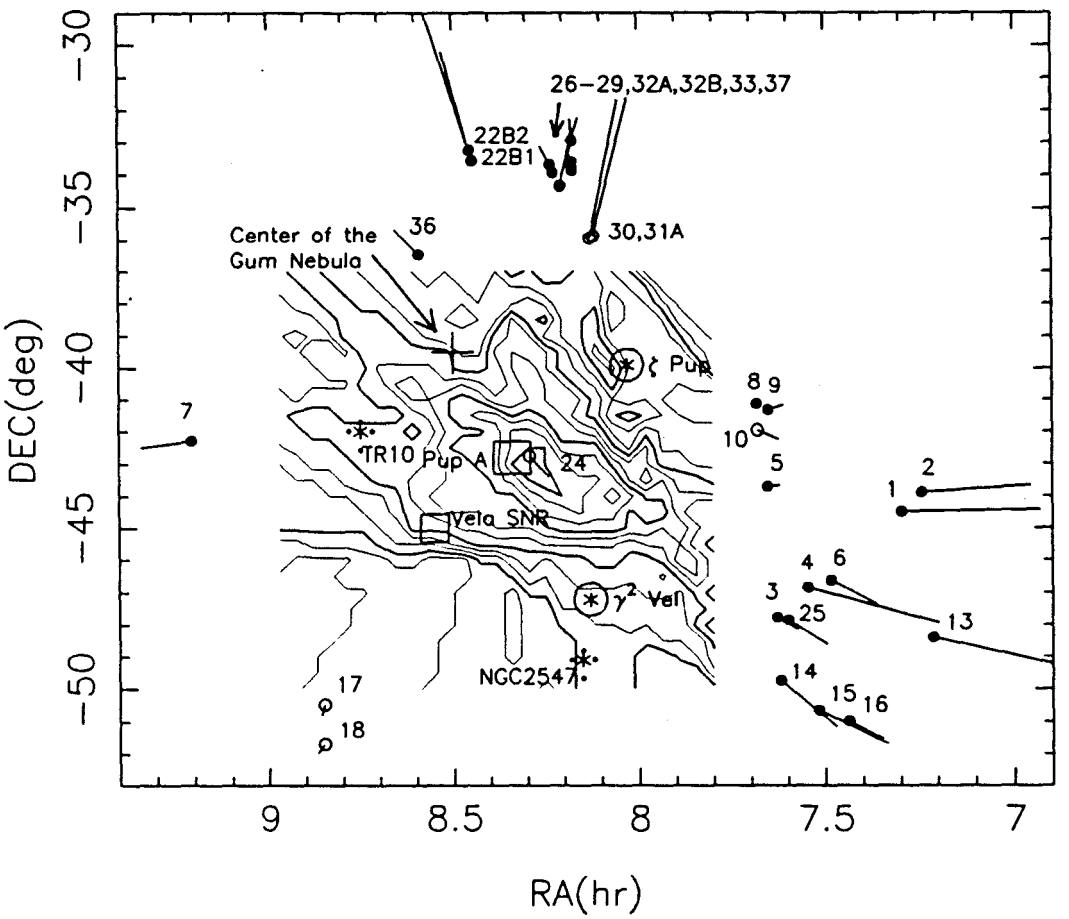

Figure 4.2: The figure shows contours of constant f, where f is the fraction of the cometary globules with position angles of their tails $\leq 10°$. The position angles are measured with respect to the line joining the head of the globule and any particular point in the region. The inner most contour bounds the region where for at least 60% of the globules the position angles of the tails are $\leq 10°$. The contours are drawn in steps of 0.05 in f and were evaluated with a grid spacing of 0.5° x 0.5". Every third contour is shown as a thick line. We designate the central maximum as the morphological center of the system. The globules used for evaluating the contours are shown as filled circles with tails, and those not used as open circles with tails. For clarity, the the tails have been scaled up 10 times. In addition, the figure shows several other interesting objects such as the Pup A SNR, the Vela SNR, ζ Pup, γ^2 Vel and the open clusters TR10 and NGC2547.

From the measured electron density of ~ 100 cm^{-3} for the bright rim of CG30 (Pettersson,1984) we estimate a recombination lifetime $t_{recomb} = (n_e \alpha)^{-1} \sim 1200$ yrs. So it is difficult to see how the presently observed bright rims can be due to the initial excitation by the supernova flash. Further. both the expansion age of the system of CGs and the age of the tails estimated in later sections are $\sim$ a few million years, thus making a causal association between Puppis A and the CGs very unlikely. We therefore conclude that the coincidence of Puppis A and tlie center is a chance superposition. On similar grounds we rule out any role for the Vela SNR in the formation of the CGs.

Figure 4.3 shows the distribution of θ_{TH}. We see that apart from the central peak there is a peak at 35° consisting of four globules, viz. CGs 26,27,29 and 33. The directions of their tails suggest that they may be associated with ζ Pup alone. It is possible that they are closer to ζ Pup in tlie direction perpendicular to the plane of the sky. Even though we cannot associate a single object of any importance with the center, we will use it as the center of the distribution of CGs for further analysis. The other objects in figure 4.2 are discussed in the next section.

4.4 Distance to the CGs

The most important objects in the region of the CGs from the point of view of momentum and energy budgets are ζ Pup, γ^2 Vel, and tlie clusters NGC 2547 and TR10. All these objects are at a distance of $\sim$ 450 pc (Eggen 1980, Claria 1982). As seen in figure 4.4, a histogram of the distances to early type stars towards the Gum Nebula used by Wallerstein, Silk and Jenkins(1980) to study gas in the nebula shows a peak at 450 pc. In an earlier study of the Gum Nebula, Brandt et *al.*(1971) had identified a possible B Association at 450 pc distance which has later been named Vela OB2. So it is clear that at a distance of 450 pc there exists a significant population of early type stars. The location of some of these objects are shown in figure 4.2. The point to note is that these objects, some of which have to be necessarily invoked to explain the CGs, are at about the sarne distance and are centrally located with respect to the distribution of CGs. So we assume that the CGs are at the same distance as these objects, viz. at $\sim$ 450 pc. Further, Pettersson(1987) has estimated a lower limit for the distance to CG30-31 complex to be 420 pc using a foreground star. and the distance to tlie young star in the head of CG1 has been estimated to be $\sim$ 500 pc (Brand et *al.*, 1983). Adopting a distance of 450 pc would imply that the distribution of the CGs extends to about 150 pc perpendicular to tho line of sight.

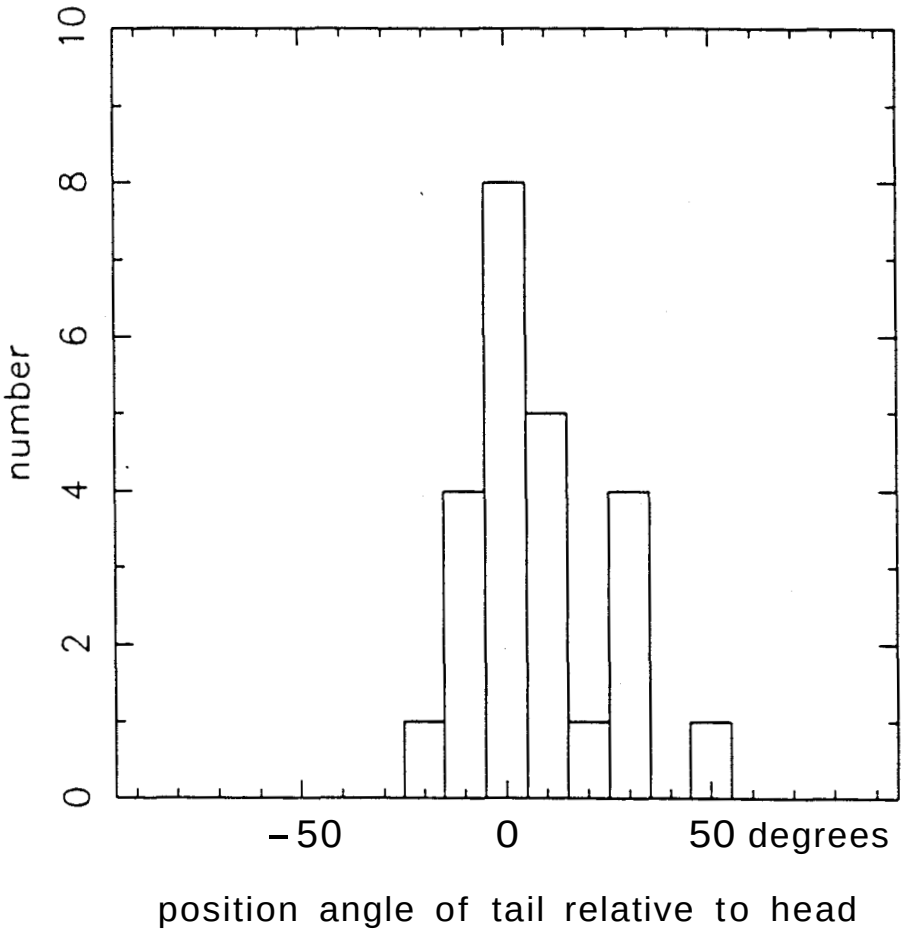

Figure **4.3:** The distribution of the position angles θ_{TH} of the tails relative to the line joining the center and the respective heads for 24 CGs (see figure 4.1).

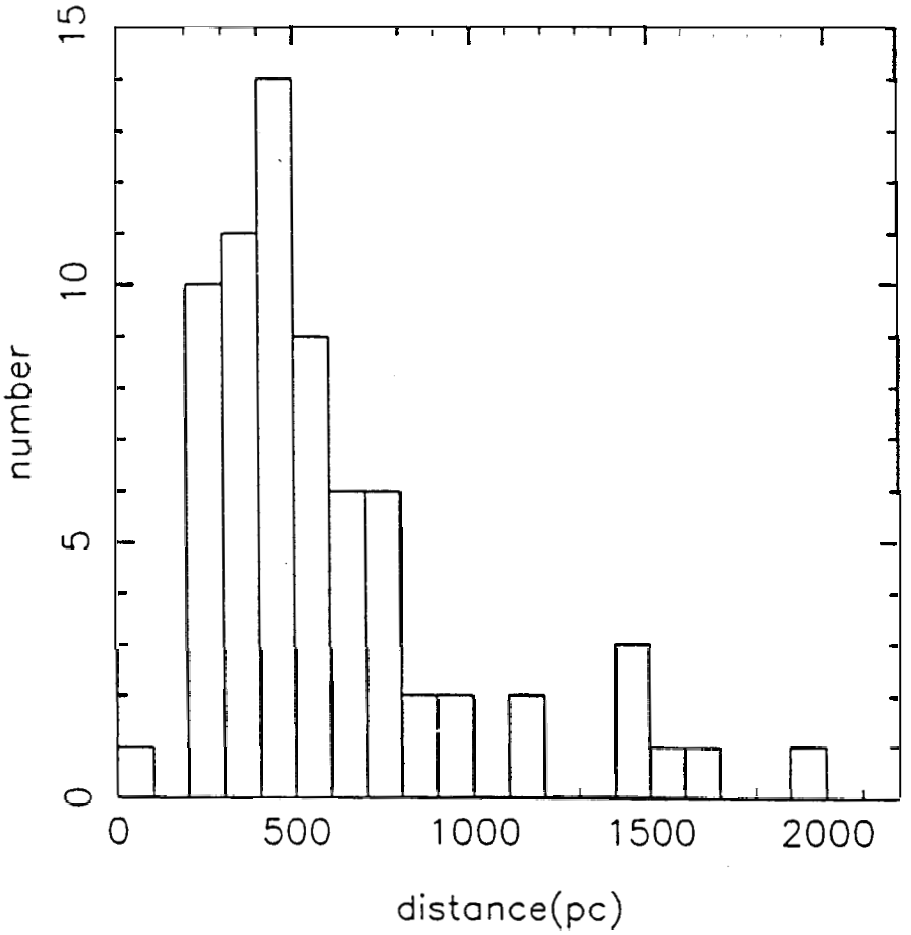

Figure 4.4: The distribution of the distances to the early type stars towards the Gum Nebula. The distances are from Wallerstein, Silk and Jenkins(1980).

4.5 Radial velocities

We now wish to discuss the implications of tlie measured radial velocities listed in Table 3.3. First, we briefly touch upon the suggestion made by Z83, viz. that the velocity distribution can be understood in terms of the large scale galactic rotation effects. In figure 4.5 we have plotted the radial velocities against the position angles of the CGs measured with respect to the *center* with zero towards north and increasing through east. The sinusoid fitted by Z83 which led them to suggest a rotation of the system of CGs is also shown. Clearly, the fit is very poor. There are two reasons why the sinusoid is a poor fit to tlie new data; (i) the revised value of the radial velocity of CG17, and (ii) velocities of CGs not detected earlier. Our main conclusion from this figure is that the model of tlie CG system rotating about an axis perpendicular to the galactic plane is untenable. In figure 4.6 we have plotted the radial velocities against galactic longtitude. Again, tlie new data does not permit a simple straight line fit as suggested earlier (Z83), and therefore an explanation based on galactic rotation effects is hard to reconcile. Nevertheless, tlie contributiori due to galactic differential rotation will be present and should be removed before attempting to interpret the velocities.

Before one can correct for the galactic differential rotation one must assume a mean distance to the CGs. Based on the discussion given in section 4, we will adopt a distance of 450 pc. The dashed line in figure 4.6 represents the expected radial velocities for different galactic longitudes from the well known formula

$$v_r = Ar \sin(2l) \cos^2 b \qquad (4.4)$$

with the heliocentric distance $r = 450$ pc and $b = 0$. We have assumed a value of 14.5 $\mathrm{kms^{-1}kpc^{-1}}$ for Oort's constant A (Kerr & Lynden-Bell 1986). The significarit deviations of the observed radial velocities from the expected value given by the dashed line suggests local motions in the CG system. Figure 4.7 shows the residuals after galactic rotation effects have been subtracted out using eq. 4.4. It sliould be remarked that the differences in the line-of-sight distances to the various globules ($\sim$ 150 pc) can only account for a scatter $\sim$ 1.4 $\mathrm{kms^{-1}}$.

4.6 Expansion of the globules

In this section we wish to argue that the velocity residuals can be easily understood in terms of an expansion of the system of globules from a common center. If tlie CGs are distributed over a shell expanding with uniform velocity then, as can be

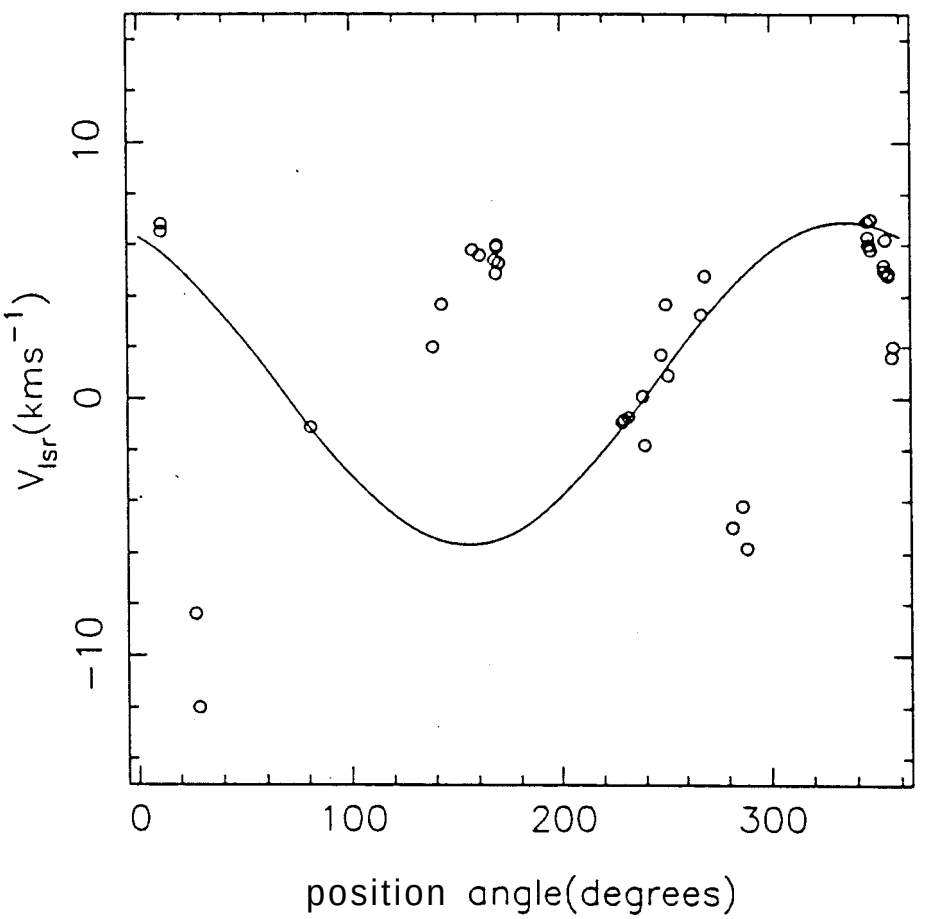

Figure 4.5: The velocities of the globules in the Gum Nebula with respect to the Local Standard of Rest. The horizontal axis is the position angle of the globules; zero is North and the position angle increases through East. The sinusoid shown is the fit made by Zealey et. *al.*(1983) for their data.

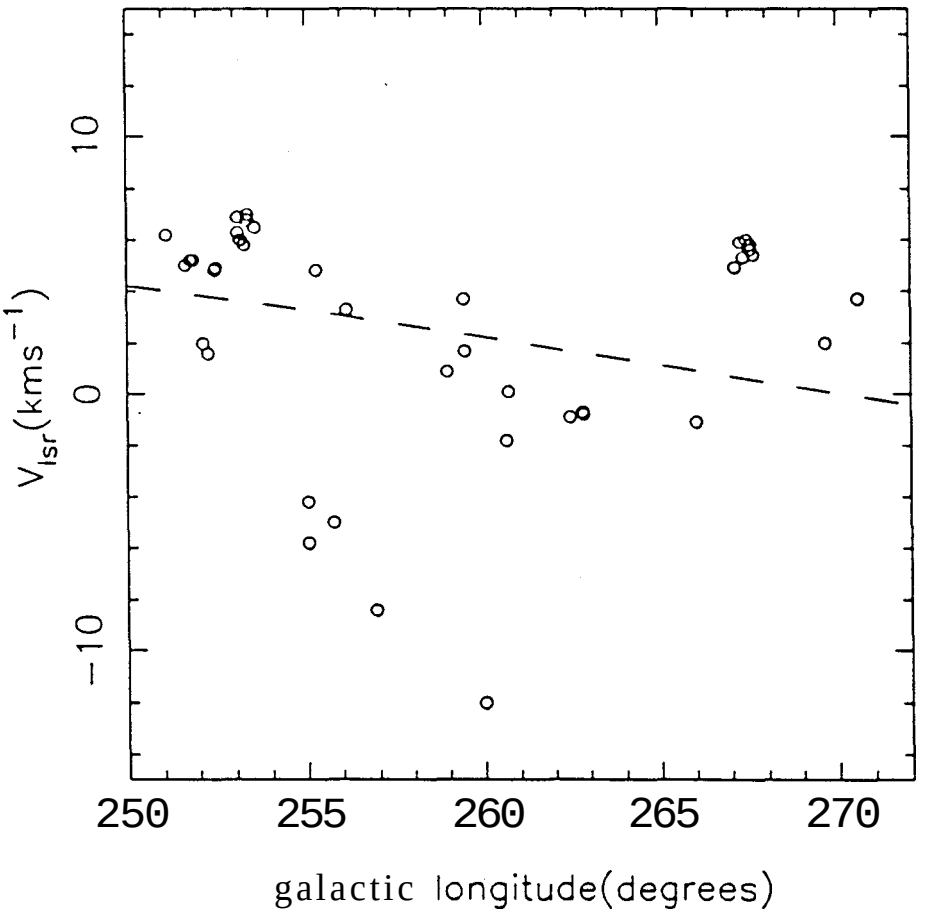

Figure 4.6: The velocities of the globules in the Gum Nebula with respect to the Local Standard of Rest versus the galactic longitude. The broken line shows expected velocities due to galactic differential rotation for an assumed heliocentric distance of 450 pc and $b = 0$.

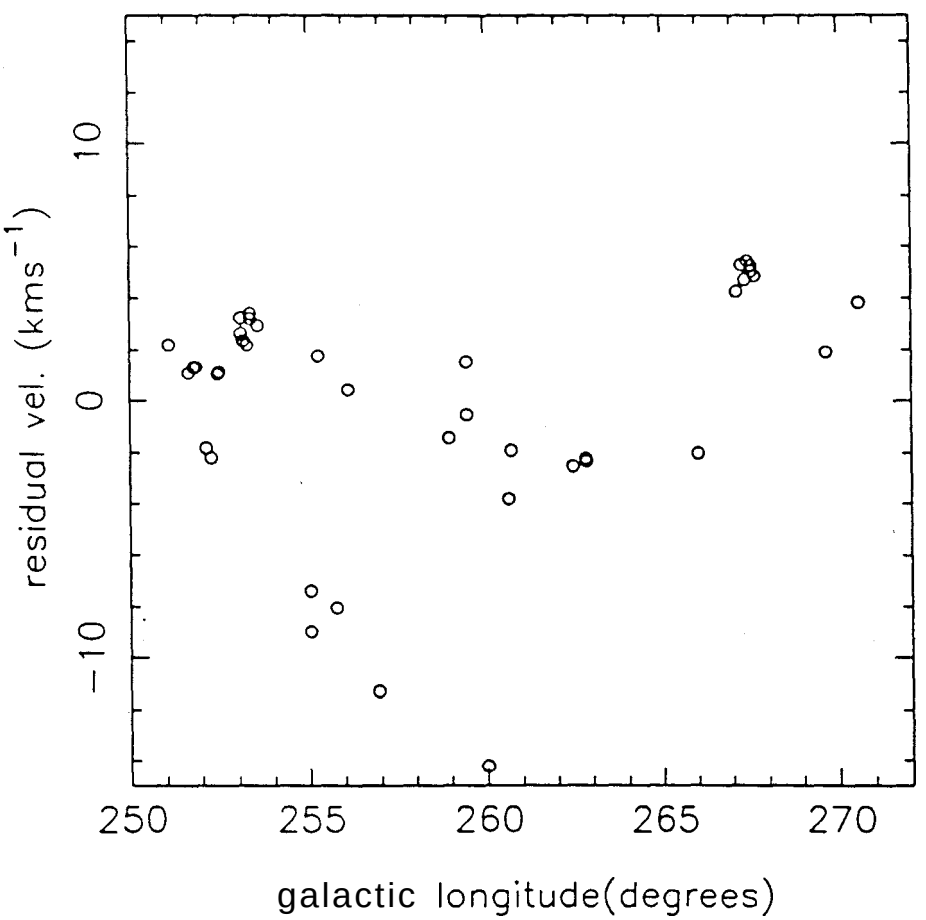

Figure 4.7: The residual velocities of the globules in the Gum Nebula after removing the contribution of the galactic differential rotation. A mean distance of 450 pc to the globules has been assumed.

seen from figure 4.8(a), the expected velocities are given by

$$v_{rad} = \pm v_{exp}(1 - \sin^2\theta/\sin^2\theta_{max})^{1/2} \quad (4.5)$$

where v_{exp} is the expansion velocity of the shell, v_{rad} is its line of sight component, and θ_{max} is the angular distance of the farthest CG from the *center*. In this case one would expect the residual velocities, when plotted against $(1 - \sin^2\theta/\sin^2\theta_{max})^{1/2}$, to fall on two straight lines as shown in figure 4.8(b). If the CGs are not on a shell but distributed throughout the sphere, then the region between the lines will be filled-up provided the inner CGs move slower than the outer CGs. If the distribution of the CGs within the sphere is not uniform one will find an incomplete filling of this region.

Figure 4.9 shows the absolute value of the residual velocities plotted against $(1 - \sin^2\theta/\sin^2\theta_{max})^{1/2}$ for all the CGs and the GDCs. We have taken θ_{max} to be 12.5°, corresponding to CG13. It is clear that there is an upper limit to the velocities which increases as one goes closer to the center (abscissa = 1) implying an expansion of the system. A contraction of the system will also have the same signature, but is very unlikely. The two straight lines shown correspond to expansion velocities of 15 kms^{-1} and 9 kms^{-1}. We will adopt an expansion velocity of 12 kms^{-1}. The figure further shows that the CGs are distributed over a volume rather than in a shell, and that the distribution is not uniform. Finally, the inferred expansion velocity of 12 kms^{-1} implies an *expansion age* of ~ 6 Myrs.

4.7 Radial velocities along the tails

In addition to measuring the radial velocities of the heads of the cometary globules, we also measured the velocities along the tails (listed in Table 3.4). In this section we discuss the results of these observations.

Out of 21 CGs for which at least three points along the tails were observed, seven show very pronounced and systematic velocity shifts. In figure 4.10 the measured velocities are plotted against the distance from the head for some of these. The velocity gradients Av, in $kms^{-1}arcmin^{-1}$ were obtained by fitting straight lines which are also shown in the figure. These gradients are also listed in Table 4.1. along with the estimated errors in the gradients. In figure 4.11 the velocity difference between the head and the extreme end of the tail is plotted against the velocity of the head for all the 21 CGs. More precisely, the ordinates are calculated as product of the velocity gradient along the tail and the tail length. The velocity differences so calculated are affected less by errors in the individual measurements. As may

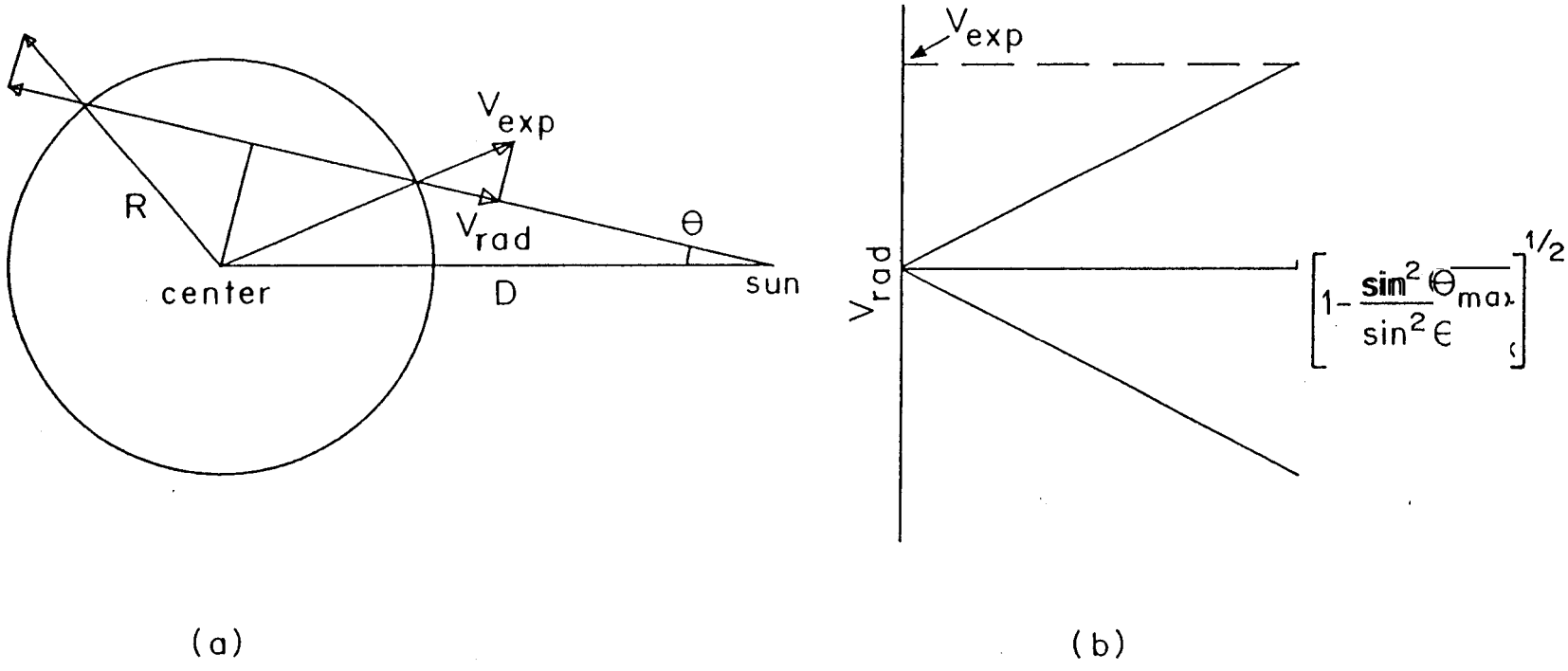

Figure 4.8: (a) A schematic diagram for deriving expected velocities from an expanding shell of objects. V_{exp} is the expansion velocity whose radial component is V_{rad} and θ is the angular distance to any point on the shell from the center of the shell. (b) The expected velocity plotted against $(1 - \sin^2\theta / \sin^2\theta_{max})^{1/2}$.

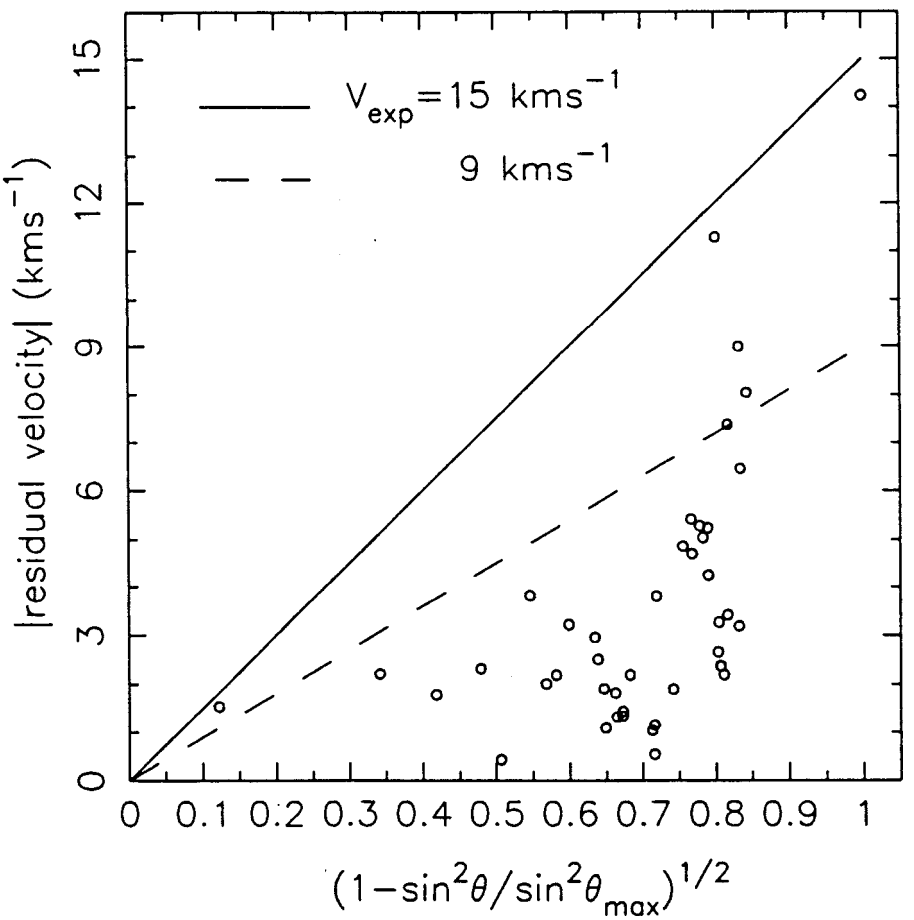

Figure 4.9: The absolute values of the residual velocities of the globules plotted against $(1 - \sin^2\theta/\sin^2\theta_{max})^{1/2}$ where 8 is the angular distance to the globule. The lines shown correspond to uniform expansion at 9 and 12 kms^{-1}

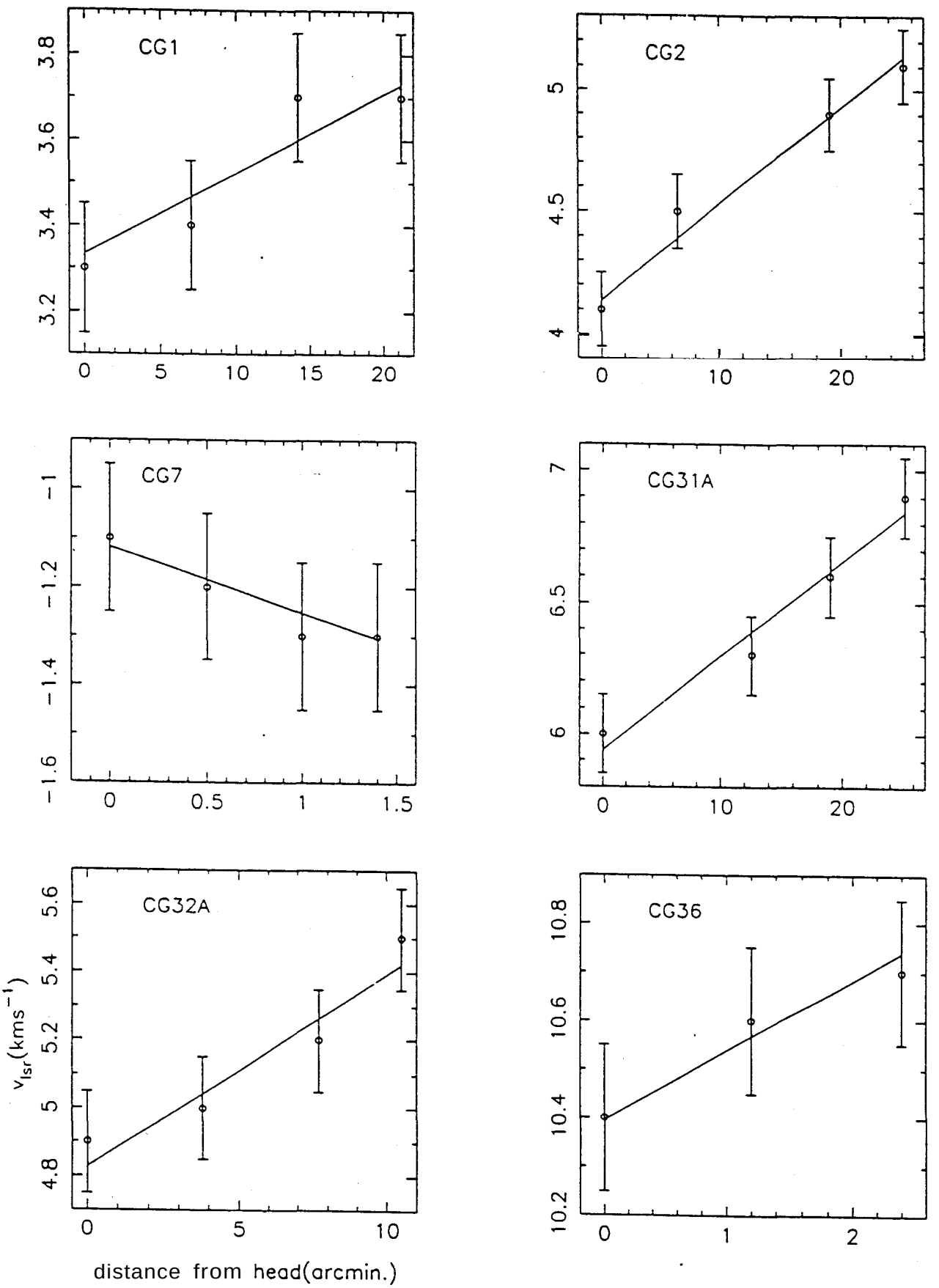

Figure 4.10: The velocity gradients along the tails for 6 out of 7 CGs which show pronounced gradients. The straight lines are least square fits to the **data** points.

Table 4.1. velocity gradients along the tails.

source	velocity gradient $kms^{-1}arcmin^{-1}$	error in gradient $kms^{-1}arcmin^{-1}$
CG1	0.019	0.003
CG2	0.040	0.004
CG3	−0.014	0.068
CG4	0.016	0.021
CG6	0.061	0.032
CG7	−0.133	0.038
CG9	0.080	0.09
CG10	−0.0.56	0.25
CG14	−0.018	0.005
CG15	−0.005	0.018
CG16	−0.018	0.013
CG24	−0.024	0.089
CG26	0.010	0.02
CG27	0.021	0.052
CG29	0.041	0.02
CG31A	0.036	0.006
CG32A	0.057	0.007
CG32B	0.114	0.043
CG33	0.082	0.032
CG36	0.144	0.05
CG37	0.017	0.064

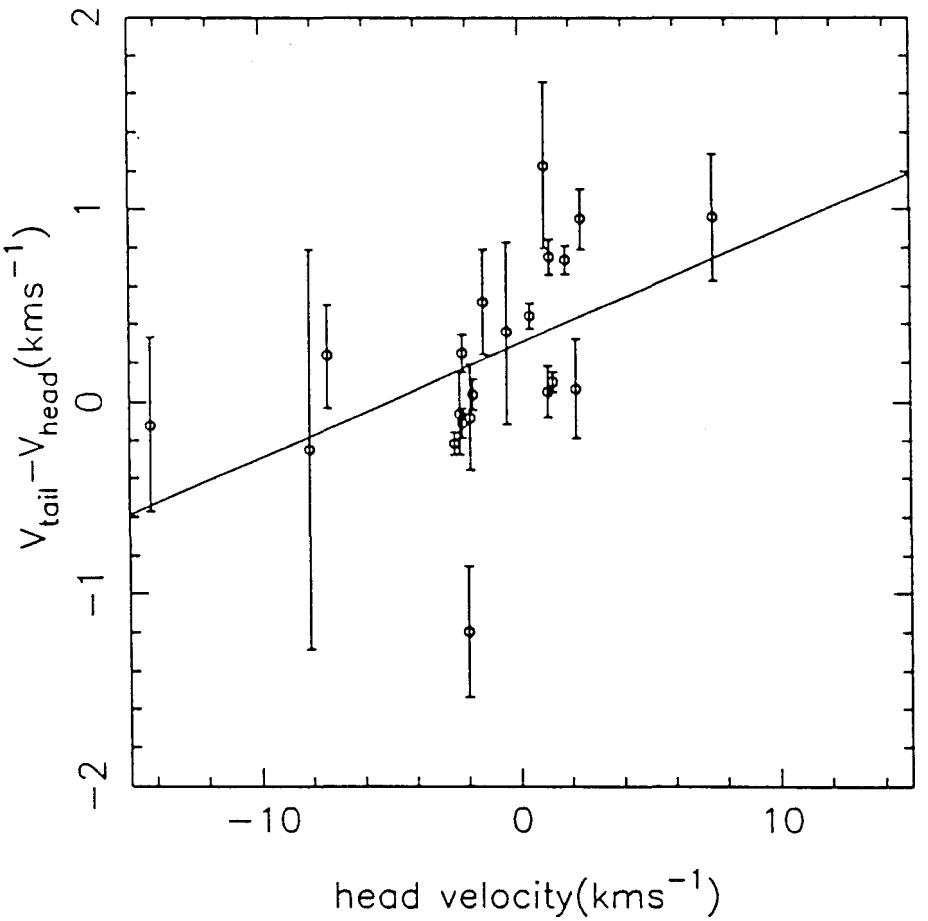

Figure 4.11: The difference in velocities between the ends of the *tails* and the respective heads plotted against velocities of the heads of the CGs.

be seen, the data points fall approximately on a straight line passing close to the origin. This implies that the gas at the end of the tails is moving faster than the heads and in the same direction as the heads.

If we assume that the tails are formed due to the stretching effect of these velocity differences over the course of time, one can calculate an age for tlic tails as tlie time taken for the presently observetl velocity difference to result in an elongation equal to the measured tail length. Since we have only tlie *radial* component for the velocity differences and the *transverse* component of the tail lengths, the calculated ages suffer from projection effects. Figure 4.12 shows the distribution of the estimated apparent ages of the tails in millions of years; a distance of 450 pc has been assumed. The apparent age is related to the real age through the relation

$$t_{apparent} = t_{real} \times \tan\theta \qquad (4.6)$$

where 9 is the angle between tlie tail and the line of sight. Since most of the CGs are distributed towards the periphery of the system, we believe that most CGs have $\theta > 45^0$. Thereore, tlie apparent age represents an over estimate of the real age. We feel that ~ 3 Myrs is a reasonable estimate for the ages of the tails.

4.8 Conclusions

From an analysis of the mesured velocities of the cometary globules we come to the following conclusions:

The kinematics of the CGs cannot be interpreted in terms of a model where galactic rotation effects dominate. as was suggested by ZS3 based on their study of a smaller sample of CGs. Our study points to two clear interpretations:

1. The distribution of the radial velocities of the heads of tlie cometary globules, after galactic differential rotation is subtracted, is best understood in terms of an expansion of the system about a common *center*. The data is better fit by a model in which the globules are non-uniformly distributed throughout the interior of a sphere, rather than in a shell. The expansion velocity of the outermost globules is ~ 12 kms^{-1}. The implied *expansion age* of the systern is ~ 6 Myr.

2. Some of tlie cometary tails show systematic velocity gradients. It is interesting that the estimated age for the formation of the tails inferred from these velocity gradients is about the same (~ 3 Myr) as the expansion age.

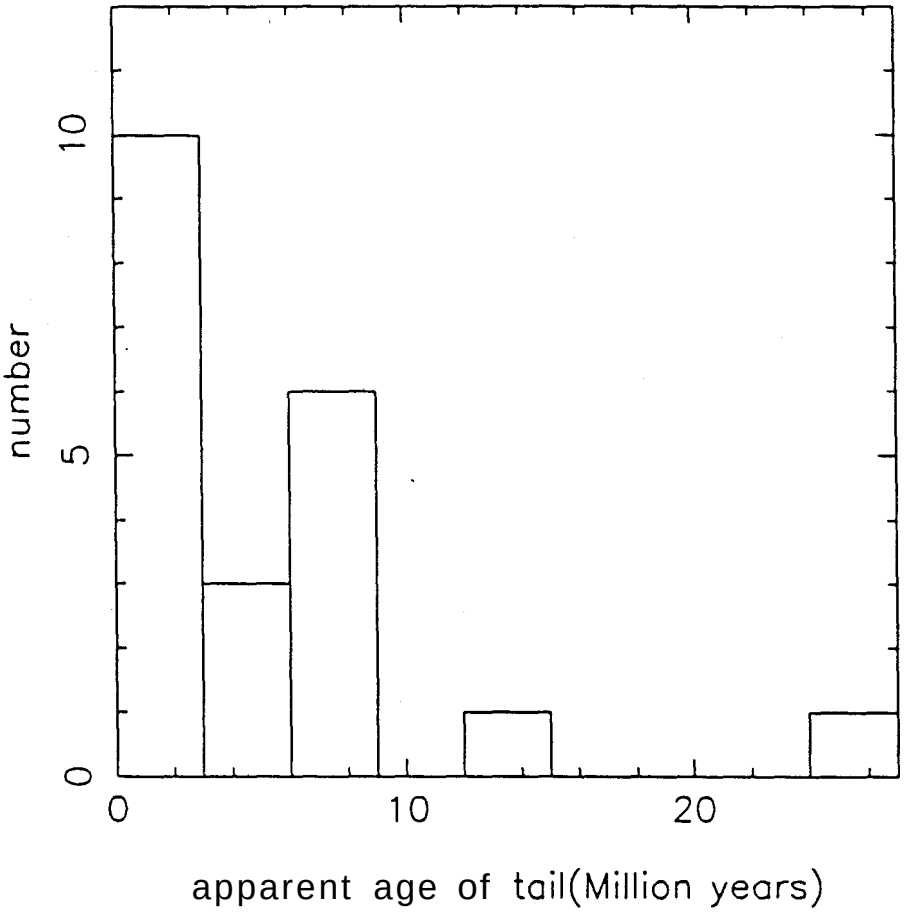

Figure 4.12: A histogram of the apparent *tail stretching ages* defined as the time required for the velocity difference between the heads and the tail-ends of the CGs to stretch the globules to their observed lengths.

REFERENCES

Brand, P.W.J.L., Hawarden, T.G., Longmore, A.J., Williams, P.M., Caldwell, J.A.R. 1983, *Monthly Notices* Roy. *Astron. Soc.*, 203, 215.

Brandt, J.C., Stecher, T.P.,Crawford, D.L.,Maran, S.P. 1971, Ay.*J.(Letters)*, 163, L99.

Caswell, J.L., Lerche, I. 1979, *Monthly Notices* Roy. Astron. *Soc.*, 187, 201.

Dubner, G.M., Arnal, E.M. 1988, *Astron. Astrophys. Suppl.*, 75, 363.

Eggen, O.J. 1980, *Ap.* J., 238, 627.

Green, D.A., 1984, *Monthly Notices* Roy. Astron. *Soc.*, 209, 449.

Kerr, F.J., Lynden-Bell, D. 1986, *Monthly Notices* Roy. *Astron. Soc.*, 221, 1023.

Milne, D.K. 1979, Aust. J. Phys., 32, 83.

Pettersson, B. 1984, *Astron. Astrophys.*, 139, 135.

Pettersson, B. 1987, *Astron.* Astrophys., 171, 101.

Smart, W.M., 1977, *Text Book* on Spherical *Astronomy*, Cambridge University Press: Cambridge.

Srinivasan, G., Dwarakanath, K.S. 1982, J. Astrophys. *Astr.*, 3, 351.

Wallerstein, G., Silk, J., Jenkins, E.B. 1980, Ay. J., 240, 834.

Winkler, P.F., Tuttle, J.H., Kirshner, R.P., Irwin, M.J., 1988, in Suyernova Rent-*nants and* the Interstellar.*Medium*, ed. R.S. Roger & T.L. Landecker(Cambridge: Cambridge University Press), p.65.

Zarnecki, J.C., Culhane, J.L., Toor, A., Seward, F.D., Charles, P.A. 1978 *Ap.* J. (Letters), 219, L17.

Zealey, W.J., Ninkov, Z., Rice, E., Hartley, M., Tritton, S.B. 1983, *Ap.* Letters, 23, 119 (Z83).